Numerical Modeling of Buckling-Restrained Braces

Mina Rizkalla, Hussein Okail, Marwan Shedid

Abstract— The BRBs' use as a lateral force-resisting system became popular in the last few decades; many existing structures do not satisfy the current seismic requirements and are vulnerable to catastrophic damage or collapse in case of future earthquakes. BRBs are commonly installed as concentric diagonal or chevron braces. This paper presents a simplified analytical approach for modeling the behavior of both individual buckling-restrained braces (BRBs) (component level) or when installed in RC frame structures (system level) when subjected to quasi-static cyclic lateral loading. SeismoStruct was used to capture the behavior at both the component level and the system level. The results of five experimentally tested individual BRBs tested by Lu et al. [1] in 2018 were used to verify the modeling approach used in the uniaxial element tests verification. The analytical models were able to capture the response of individual BRBs. Truss elements were utilized to represent the brace elements, and values for the parameters controlling the cyclic behavior of the used brace steel material model were recommended. The macro model for the BRB was incorporated at the system level, which enhanced the in-frame seismic behavior knowledge. Accordingly, its seismic behavior prediction could be possible. The maximum mean errors achieved for the BRB ultimate strength at the component and the system levels were 5% and 4.7%, respectively. This study aims to perceive proper modeling techniques that could be useful to carry out further parametric studies, either on individual BRBs or in-frame structures retrofitted with BRBs.

Index Terms— Buckling-Restrained Braces, Numerical Modeling, Pushover analysis, RC frame, Target displacement.

1 Introduction

Buckling-restrained braces (BRBs) are seismic force-resisting elements, behaving as visco-elastic dampers to dissipate energy in compression as well as in tension.

To attain a more optimal elastoplastic behavior. The brace buckling is restrained by external means and, the core yields. Symmetric behavior is obtained at both tension and compression sides; as the axial force is decoupled, with a difference up to 10% larger for the compressive strength [2].

As concentrically braced frames (CBF) design members result in huge sections due to the buckling effect. However, in BRBs design, as the buckling is not permitted, this results in slender cross-sections. Commonly used BRBs are composed of:

i) Steel core; the steel core can be either a single flat plate or multiple of a crucified cross-section; it is made of ductile steel and can resist forces at adjusted strengths in compression as well as in tension. The steel core is divided into three segments; the first is the restrained yielding segment. The second is the restrained non-yielding transition segment. And this part is an extension to the first segment but with added stiffeners to increase the cross-section to ensure the elastic behavior. The third segment, which is the un-restrained, non-yielding segment, is an extension of the second segment and extends outside the casing [3], [4]. This segment is the part that is connected to the frame. Concerning the frame connection, it can be bolted, welded, or pinned connection [5]. These core segments must achieve appropriate stiffening to prevent such failure. On the other hand, if the gap is not sufficient or not provided, the lateral supporting system will withstand the load and, the brace's middle length may fail against buckling.

ii) Casing (buckling-restraining system) can also be called "Restrainer"; this casing may be steel, concrete, composite, or any other material. Also, the casing can be square or circular shaped. It is usually hollow square section (HSS). This casing restrains the overall buckling and offers its lateral stiffness when the core laterally deforms.[6]

iii) De-bonding material/insulator; it can be grease, silicon rubber sheets, vinyl sheets, masking tape, extruded polystyrene foam, asphalt paint, or an air gap. It is placed around the core to provide a space and prevent bonding between the core and the casing to lessen the friction force. Therefore, no axial load is transferred to the casing and is resisted only by the yielding steel core. [7], [8]

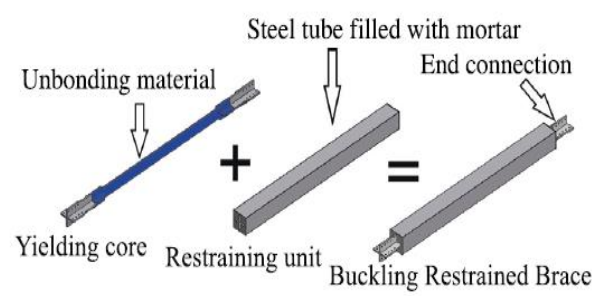

Fig. 1. Schematic description of the conventional BRB (Pedrafit et al., 2013) [8]

1.1 BRB Merits

BRBs have many advantages among these advantages that they do not experience the disadvantages of the conventional

- *Mina Rizkalla, postgraduate student, School of Engineering, Ain Shams University.* minarizkalla@eng.asu.edu.eg
- *Hussein Okail, Professor, School of Engineering, Ain Shams University.* hussein.osama@eng.asu.edu.eg
- *Marwan Shedid, Professor, School of Engineering, Ain Shams University.* marwan.shedid@eng.asu.edu.eg

braces as buckling is eliminated. Buckling-restrained braced frames (BRBFs) lateral stiffness is better than that of moment-resisting frames (MRFs). They are high-energy dissipation elements, as the strains are not concentrated in a limited region like a plastic hinge, accordingly, the braces can dissipate a large amount of energy. BRBFs have almost balanced/symmetric hysteretic behavior in both tension and compression. That results in the core area size, which could be determined from the design level seismic loads based on the core yield stress.

Among the aesthetic advantages, BRBs have small sections as buckling is not permitted, smaller beams and columns sections due to lower seismic demand, require smaller and simpler connections. Consequently, less required seismic loads, less seismic damages, and therefore, lower losses; as the other structural members' damage decreases, and also lower forces on foundation, so cheaper one.

Concerning the erection advantages they are easy and fast erected, easy to install in seismic retrofitting, and easy post-earthquake investigation and replacement [9].

1.2 BRB Applications

The BRBs are widely used worldwide in the last few decades, and here are some of their applications [3], [6], [10]

i) Grand Tokyo; A 205 m high, 43 story building located in Tokyo, Japan. The building, finished in 2007, is an example of high rise built BRB application structure.

The following example is a Grid Skin Structure using BRBs. Grid Skin structures use vertical and diagonal perimeter members, forming the main seismic and wind resisting frame, including the "Brace Tube" and "Diagrid" concept systems [11].

ii) 181 Fermont Tower; A 205 m high, 56 story building located in San Francisco, USA. This building is covered by mega braces utilizing BRBs and viscous dampers; this system provides damping equivalent to 8%.

The following example is a retrofit work for a communication Tower. BRBs can also be used to retrofit truss structures (replace the weak/insufficient strong members with BRBs). [11]

iii) Communication Tower; the communication tower is located in Japan, on the top of a building roof; such towers suffer from risks of collapse during severe earthquakes, so they are retrofitted [12].

2 Literature Review

Yooprasertchai et al. [13] conducted a quasi-static cyclic load experimental test on a non-seismic detailed frame; the study purpose was to examine the availability of applying BRBs to low-rise non-ductile RC buildings. The concept of retrofitting is based on reducing the inelastic deformation demand of the non-ductile existing building components (e.g. Columns) and enhancing the building energy dissipation capacity.

The research found that the diagonally assembled BRB to the RC column behaved well in both the tension and compression, and showed good stable ductile cyclic loops. The connections with the chemical anchor studs were able to bear the cyclic load. The existence of BRB in the frame increased the energy dissipation by increasing the stiffness and strength.

Sarno et al. (2008) [14] conducted a comparative nonlinear time history analysis (THA) between BRBs (concentric braces) and rigid tension-compression braces mounted in concentric arrangements as found in exterior mega-brace format. Six different ground motion records were carried out for the THA.

A 30% reduction in the interstory drift, using the concentric braces, was found, while a 50-60% reduction was provided by the mega braces. Also, BRBs have superior performance. However, they are more complex and have greater weight when compared to mega braces, which have less weight (about 20% less total steel amount), leading mega bracing to have less construction cost.

Bordea and Dubina (2009) [15] tested the BRB effectiveness to retrofit a non-ductile RC three-story building. A nonlinear static pushover analysis was conducted prior to adding the BRBs using the SAP2000. Chevron bracing was inserted along the central bays of the outer perimeter of the building in both directions.

The analytical study indicated that for the original building, some plastic hinges were formed in the columns followed by the beams, while for the retrofitted building, the formation of the plastic zones started in the BRBs followed by the columns and beams. Members strengthening increased the overall strength 2.5 times, and decreased the top displacement to quarter its former value. The research study recommended better BRB sizing to match the expected strength and demands. As a result of adding new braces, it was also recommended to consider local FRP strengthening of the beams and columns to deal with the increased strength.

Skokan et al. (2010) [16] conducted a nonlinear analysis; to evaluate RC MRF 6-story building seismic retrofitting performance. The study's retrofitting plan was adding new exterior RC frames beside that of the existing ones. The new frames included BRBs mounted in chevron type; the newly added RC frames were linked with the existing structure using epoxy dowels. A 3D SAP2000 model was generated to confirm the seismic performance of the retrofitting plan, a group of 7 scaled ground motion records was utilized in the THA, as the aim of the retrofitting strategy is to offer the required strength, stiffness, and ductility upgrade while exposing to heavy earthquake activity.

It was concluded from the analysis that the maximum story drifts were reduced to 0.8%, and also, the deficient MRF force demands were reduced by 70% of the total base shear forces.

Qu et al. (2015) [17] conducted a research on a 12 story building retrofitted with single diagonal BRBs in a zigzag manner. The research program utilized the ABAQUS software program; this prototype model was used to study the behavioral effect of the brace connection and tested under three different ground motion records.

It was concluded that the effect of BRB connection nonlinearity is being assessed through the non-linear THA. The interstory drift of the entire building increased by increasing the flexibility of concrete corbels.

Pan et al. (2016) [18] conducted an experimental study on a one-bay RC frame structure. The frame is a part of an old Taiwanese school building; the building is deficient and does not cope with the Taiwan seismic standards of nowadays. The

research program was to try a load transfer mechanism through a load-bearing block.

The feasibility of the suggested method was deduced; the design predictions well matched with the experimental behavior; as the seismic energy was dissipated mainly through BRB yielding, plastic hinges formation at both ends of the RC columns and steel frame. The BRBs in the retrofitted frames showed a good performance with stable and repeatable hysteretic behavior that could be computed about 56% of the total lateral resistance. The cracking failure of the bearing blocks could be resisted by wire mesh reinforcing, enhancing the load transfer as well as the retrofitted frame overall ductility and serviceability.

Abou-Elfath et al. (2017) [19] conducted a numerical analysis using the SeismoStruct software on a rectangular plan six-story building; the building is composed of solid slabs and MRFs in both directions to resist the seismic force. The BRBs were designed in the research study to resist; 50%, 100%, and 150% of the base shear capacity of the original RC structure. The structure was retrofitted with single diagonal BRBs at one bay on each side on the outer perimeter of the building. The perimeter frames experienced an increase in the axial load. Thus they were jacketed to increase their axial capacity. The structure was seismically evaluated by conducting static pushover and THA.

It was concluded that using BRBs in a single diagonal form is a significant way to resist the base shear of RC structures. Also, lead to decreasing the story drifts, the fundamental periods, beam, column, and brace ductility strain factors.

3 Uniaxial Element Validation (Phase I)

The modeling validation is carried out using the SeismoStruct v2020 [20] FE software computer program. The validation goes through two phases, the first one is the "Uniaxial Test Verification"; single BRB elements are subjected to displacement control phases, the reference specimens were tested experimentally by Lu et al. 2018 [1]. After validating these elements in a single manner (component level), they will be used in modeling and validating whole RC frames retrofitted with BRBs (system level) in the latter phase.

3.1 Specimens Geometry

Five single BRB elements are demonstrated in **Table 1**, are subjected to reversed cyclic loading; the loading protocol is variable for each brace. The variation of the loading protocol, adopted in the experimental program and demonstrated in **Fig. 2**, was for some project requirements.

3.2 Material Models

The brace element is modeled as an "Inelastic truss element" class and discretized into 200 section fibres. The material used to model the brace element is that proposed by the program "Buckling Restrained Steel Brace model" (stl_brb), to complete defining the BRB steel material behavior, eleven parameters for the steel characteristics must be inserted in the FE program. offers these parameters along with their calibrated values. While the values for the material properties from the experimental coupon tensile tests carried out to determine the actual material properties for each BRB specimen are summarized in **Table 1**

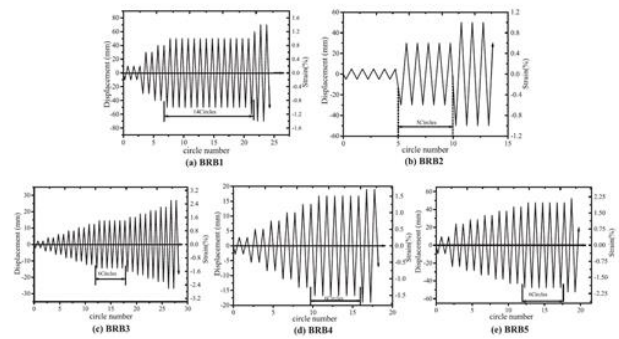

Fig. 2 Loading history for the five BRB specimens (Lu et al.,2018)

Table 1
BRB Specimens Geometry and Material Properties Summary (Lu et al. 2018.).

Specimen	Core (mm^2)	L_y (mm)	Yield Strength f_y (MPa)	Ultimate Strength f_u (MPa)	Elastic Modulus E (MPa)
BRB1	150x25	5083	249	418	2.04×10^5
BRB2	150x25	5083	305	443	2.1×10^5
BRB3	150x25	1035	291	452	2.1×10^5
BRB4	80x10	1120	267	440	2.01×10^5
BRB5	70x12	2386	304	448	1.96×10^5

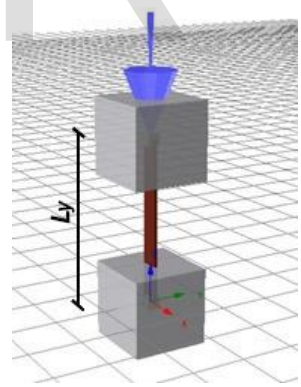

Fig. 3 Numerical single BRB element model

The braces are of rectangular cross-section, so the rectangular solid section (rss) is utilized while modeling the braces' cross-sections. The section dimensions are variable and determined according to each specimen, and their geometries are also summarized in **Table 1**. The single brace element is modeled using only two nodes; the lower one is restrained in both the X and Z-directions, while the upper is restrained only in the X-direction [21], [22].

TABLE 2
THE "STL_BRB" MATERIAL UTILIZED VALUES.

Parameter	Value
Constant Controlling elastic to plastic transition for tension	0.40
Hardening ratio for tension	0.014
Constant Controlling isotropic hardening for tension	0.5
Constant Controlling elastic to plastic transition for compression	0.30
Hardening ratio for compression	0.01
Constant Controlling isotropic hardening for compression	0.20
Specific weight (N/mm³)	78.00

3.3 Individual BRBs (Phase I) Analytical Results

In comparison to the experimental data, the cyclic load-displacement relationships for the uniaxial BRB elements from phase I show a good agreement with the experimental hysteresis loops results for the positive portion (push test) and acceptable results for the negative one (pull test). The model can predict the most important characteristics of the BRB cyclic response like hysteresis loops, ultimate strength, stiffness degradation, and energy dissipation.

A comparison was conducted between the analytical and experimental results; the comparison comprises hysteretic shape/cyclic response, skeleton curves, peak strength, effective stiffness, and energy dissipation. The "% Difference" could be a measuring tool for the evaluation process, and it is the difference between the analytical and experimental mean values to the experimental ones; where the mean value is the average of both the absolute positive (push) and negative (pull) captured parameter values.

$$\%\,Difference = \frac{Analytical\ mean\ value - Experimental\ mean\ value}{Experimental\ mean\ value} x100$$

For specimens BRB1 - BRB4, the positive portion of the loops or the skeleton curves fit better than the other portion with a lesser difference from the experimental results. Specimen BRB3 shows a very good agreement with the experimental results; the average difference for the positive portion is observed not exceeding 1.2%, while the detected negative portion difference was about 10%. For specimen BRB5, the mismatching of the last cyclic loops may come from the out-of-plane failure of the specimen due to insufficient test setup constraints.

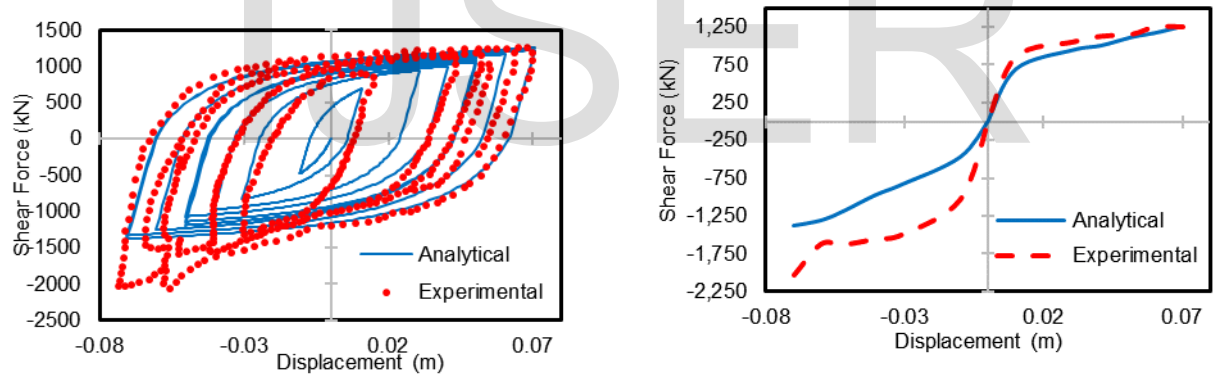

(a) Specimen BRB1 Hysteresis Loops and Push-Pull Envelopes

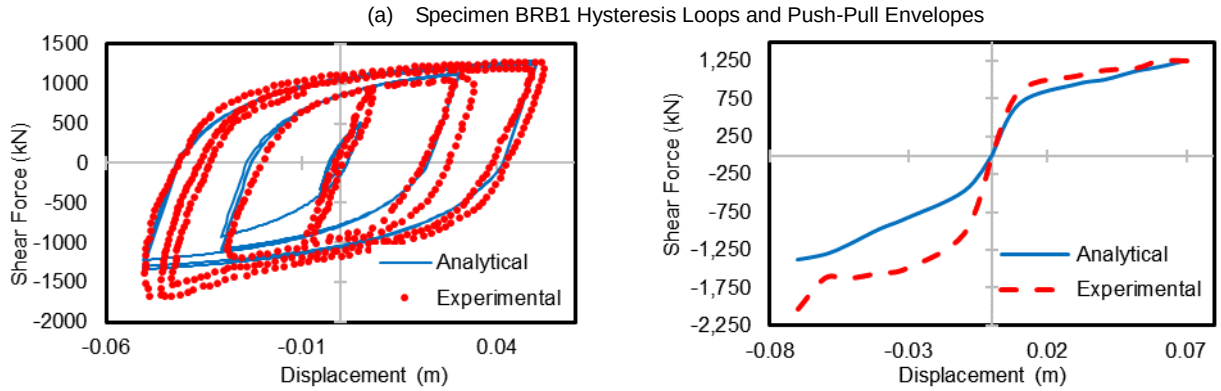

(b) Specimen BRB2 Hysteresis Loops and Push-Pull Envelopes

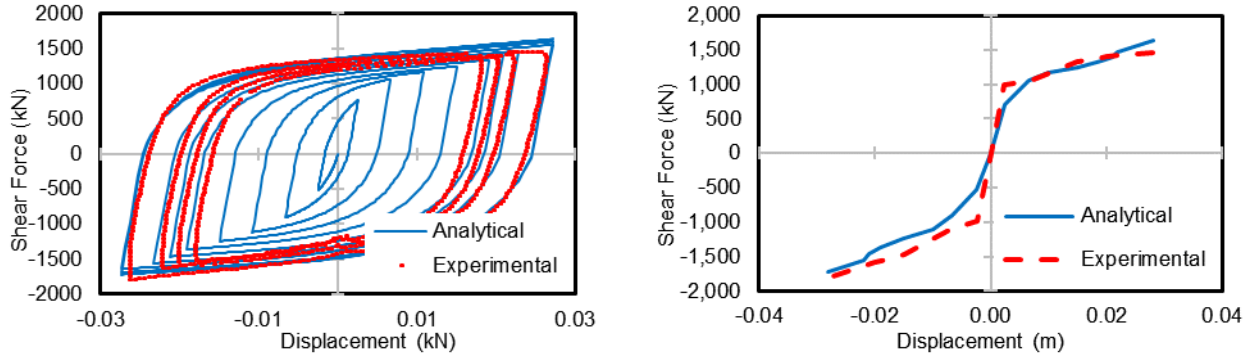

(c) Specimen BRB3 Hysteresis Loops and Push-Pull Envelopes

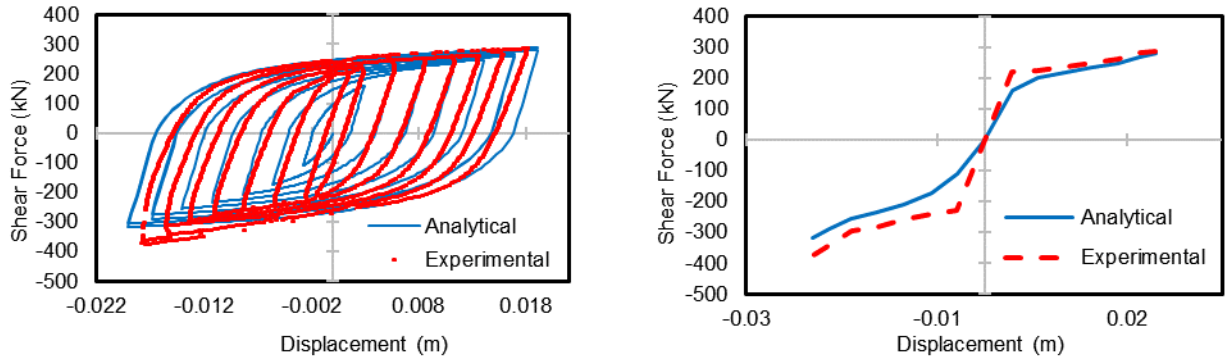

(d) Specimen BRB4 Hysteresis Loops and Push-Pull Envelopes

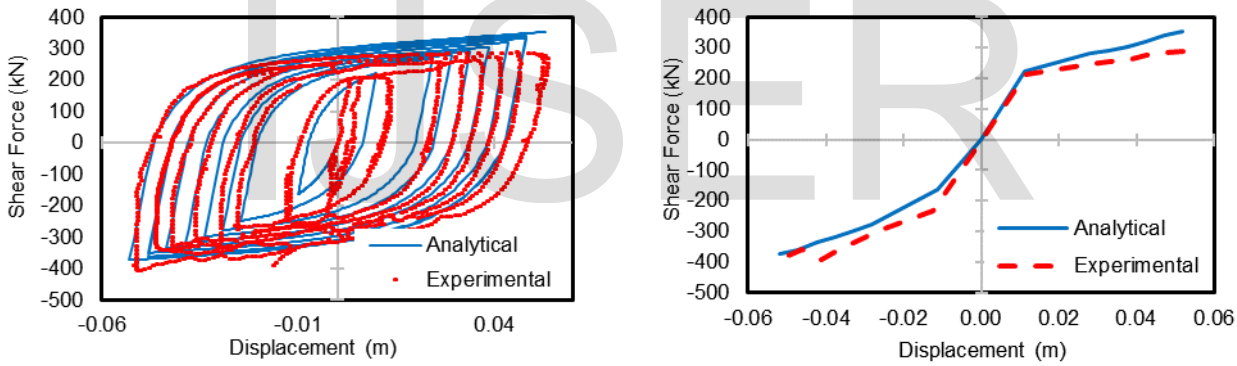

(e) Specimen BRB5 Hysteresis Loops and Push-Pull Envelopes

Fig. 4 BRB Specimens Validation

TABLE 3 demonstrates the difference among experimental and analytical values for the ultimate shear force, Qu. As well, the average difference among the measured experimental and analytical values for shear force for all the five specimens is detected to be 5%.

The model can capture the ultimate strength of the elements in a good manner, with a maximum mean difference of 9%, excluding the 19% of BRB1, as specimen BRB1 in the experimental program; was subjected to various amplitudes of displacement; for testing its fatigue properties. For the first specimen, an apparent end rotation was observed at its lower end, causing friction abrupt between the restraining member and the core; therefore, the BRB compressive force exceeded 2000 kN. This behavior is analytically avoided, and the hysteretic behavior is almost similar on the tension side as well as on the compression side. So that is why the negative portion of the skeleton curves does not coincide.

TABLE 4 demonstrates the comparison among the experimental and analytical values for the displacement at ultimate shear strength.

TABLE 3 SUMMARY OF EXPERIMENTAL AND ANALYTICAL ULTIMATE SHEAR FORCES

Specimen	Experimental (kN)			Analytical (kN)			Diff.
	Q_{u+ve}	Q_{u-ve}	Mean	Q_{u+ve}	Q_{u-ve}	Mean	
BRB 1	1265	-2069	1667	1284	-1418	1351	-19%
BRB 2	1274	-1670	1472	1309	-1369	1339	-9%
BRB 3	1463	-1786	1624	1632	-1721	1677	3%
BRB 4	287	-371	329	289	-317	303	-8%
BRB 5	291	-405	348	359	-379	369	6%

TABLE 4 SUMMARY OF EXPERIMENTAL AND ANALYTICAL DISPLACEMENTS AT ULTIMATE SHEAR STRENGTH

Specimen	Experimental (m)			Analytical (m)			Diff.
	Δ_{u+ve}	Δ_{u-ve}	Mean	Δ_{u+ve}	Δ_{u-ve}	Mean	
BRB1	0.069	-0.056	0.063	0.071	-0.071	0.071	13%
BRB2	0.050	-0.052	0.051	0.050	-0.051	0.050	-1%
BRB3	0.026	-0.030	0.028	0.027	-0.027	0.027	-3%
BRB4	0.018	-0.018	0.018	0.019	-0.019	0.019	8%
BRB5	0.052	-0.051	0.052	0.053	-0.053	0.053	2%

The captured ultimate strength force by the program is not so far from that of the experimental program, with a maximum mean difference of 1.5% for all specimens excluding the first one. For the first specimen, the captured analytical displacement at the ultimate strength was for the last cycle and maximum amplitude, while its corresponding experimental one is not at the same location because of the experienced end rotation by this specimen causing an abrupt increase in the resisting force, such behavior is not modeled, and here the relatively large difference is comprehended.

3.3.1 Effective Stiffness

The effective stiffness (k_{eff}) is calculated as per ASCE 7-10 [23] through the following equation to assess its variation with the increased displacement.

$$keff = \frac{|F^+| + |F^-|}{|\Delta^+| + |\Delta^-|}$$

Where F^+ and F^- are the positive and negative shear resistance of the brace element at Δ^+ and Δ^- respectively, and Δ^+ and Δ^- are the maximum push and pull displacement for each cycle. The analytical versus the experimental result curves are demonstrated below in Fig. 5 (a) with an average difference of 13.8%.

3.3.2 Energy Dissipation

The Energy dissipation Ed is an important factor in seismic design, as it diminishes the seismic response. Some previous researches [24] revealed that the Ed represented as the area enclosed by the envelope of the hysteretic curve is not sensitive to accurately assess the response of the enforced displacement increments. The Ed is represented according to Hose and Seible (1999) [25] as the area enclosed by the envelope curves of cyclic loops. The mean difference reached from comparing the analytical and experimental results was 19%.

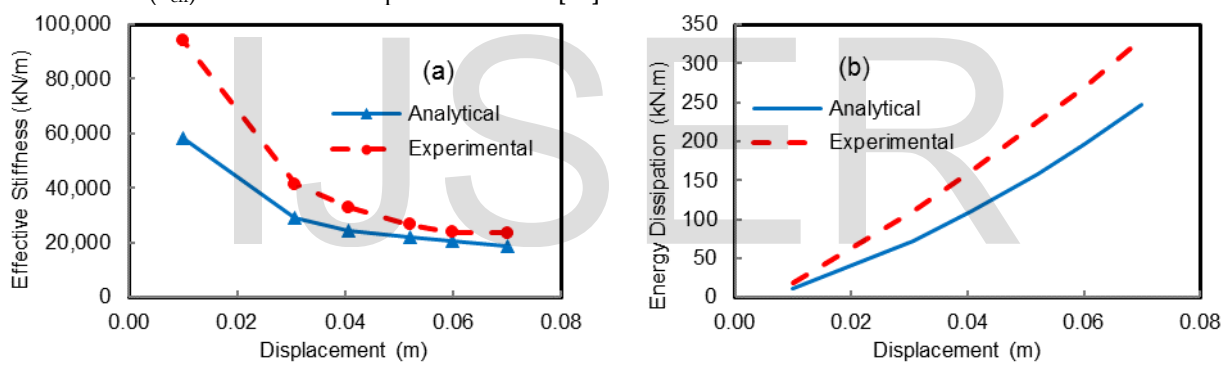

Specimen BRB1

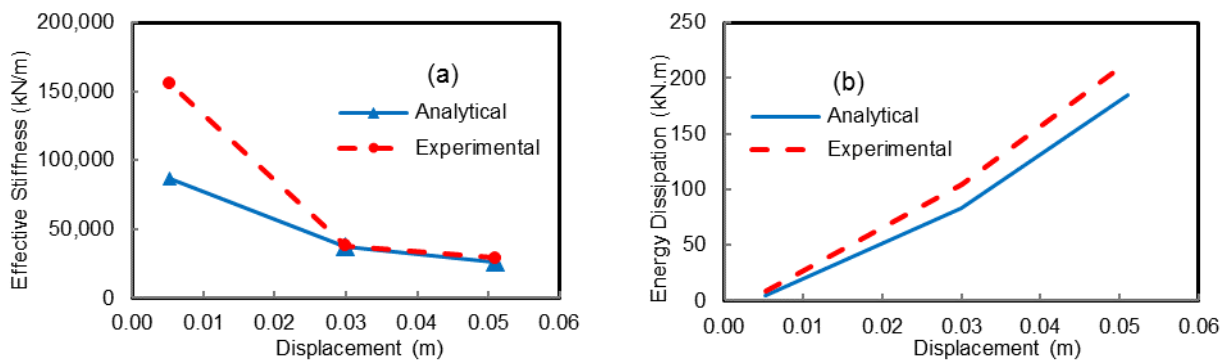

Specimen BRB2

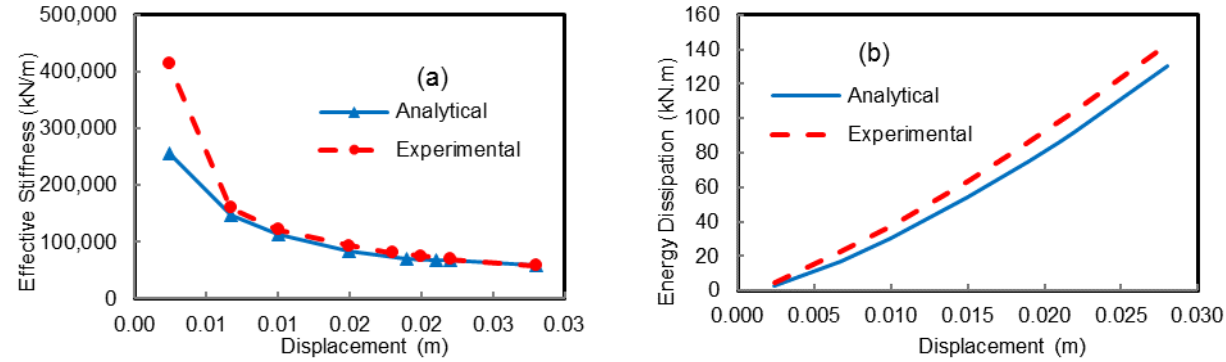

Specimen BRB3

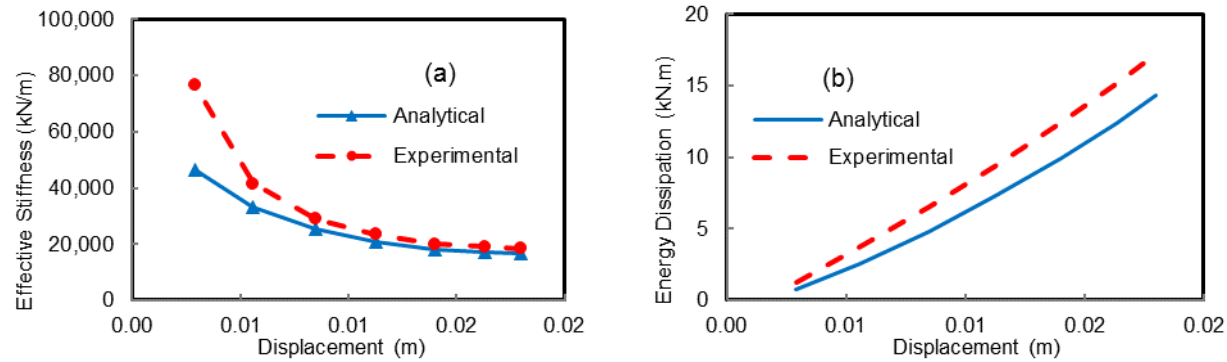

Specimen BRB4

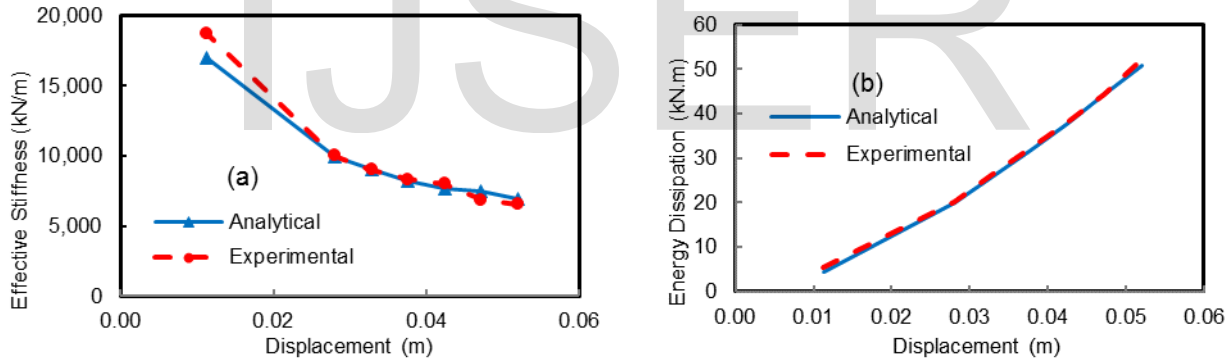

Specimen BRB5

Fig. 5 Analytical vs Experimental Stiffness and Energy Dissipation Results
(a) Effective Stiffness; and (b) Energy Dissipation

Displacement (m)	Specimen BRB1					
	Stiffness (kN/m)			Energy Dissipation (kN.m)		
	Analytical	Experimental	Difference	Analytical	Experimental	Difference
0.07	18821	23521	-20%	11.63	18.86	-38%
0.06	20627	23892	-14%	72.41	110.51	-34%
0.052	22122	26743	-17%	109.53	162.19	-32%
0.0406	24330	32981	-26%	158.28	224.42	-29%
0.0307	28884	41395	-30%	196.48	269.61	-27%
0.01	58142	94300	-38%	247.59	331.21	-25%
		Average	-24%		Average	-31%

Displacement (m)	Specimen BRB2					
	Stiffness (kN/m)			Energy Dissipation (kN.m)		
	Analytical	Experimental	Difference	Analytical	Experimental	Difference
0.051	25735.05	28867.16	-11%	25735.05	28867.16	-11%
0.03	37388.27	37654.33	-1%	37388.27	37654.33	-1%
0.0052	86924.04	155805.10	-44%	86924.04	155805.10	-44%
		Average	-19%		Average	-19%

Displacement (m)	Specimen BRB3					
	Stiffness (kN/m)			Energy Dissipation (kN.m)		
	Analytical	Experimental	Difference	Analytical	Experimental	Difference
0.028	59883.34	58135.00	3%	2.95	4.77	-38%
0.022	68730.45	69696.82	-1%	16.72	22.55	-26%
0.02	68165.05	74722.25	-9%	30.73	37.62	-18%
0.018	71065.95	80864.17	-12%	54.55	63.73	-14%
0.015	82967.10	93333.33	-11%	75.31	80.86	-7%
0.01	113739.90	121111.50	-6%	86.44	92.66	-7%
0.0067	147104.55	160032.84	-8%	92.32	104.77	-12%
0.0024	256319.58	414352.08	-38%	130.59	142.71	-8%
		Average	-10%		Average	-16%

Displacement (m)	Specimen BRB4					
	Stiffness (kN/m)			Energy Dissipation (kN.m)		
	Analytical	Experimental	Difference	Analytical	Experimental	Difference
0.018	16592.22	18325.33	-9%	0.78	1.29	-40%
0.0163	17151.78	19155.21	-10%	2.52	3.75	-33%
0.014	17882.46	19964.04	-10%	4.84	6.54	-26%
0.0113	20644.69	23508.63	-12%	7.34	9.41	-22%
0.0085	25163.00	29030.88	-13%	9.95	12.35	-19%
0.0056	33262.32	41591.70	-20%	12.39	15.07	-18%
0.0029	46483.79	76841.90	-40%	14.36	17.25	-17%
		Average	-16%		Average	-25%

Displacement (m)	Specimen BRB5					
	Stiffness (kN/m)			Energy Dissipation (kN.m)		
	Analytical	Experimental	Difference	Analytical	Experimental	Difference
0.052	6973.02	6539.68	7%	4.31	5.30	-19%
0.0472	7451.35	6870.93	8%	20.08	20.18	-1%
0.0424	7713.94	8011.75	-4%	25.59	26.02	-2%
0.0376	8264.57	8322.28	-1%	31.41	31.92	-2%
0.0328	9003.52	9045.89	0%	37.53	37.94	-1%
0.028	9961.63	10019.52	-1%	44.05	44.39	-1%
0.01125	17037.07	18757.18	-9%	50.90	52.12	-2%
		Average	0%		Average	-4%

4 In-Frame Test Validation (Phase II)

The second phase is the "In-frame Test verification"; the purpose of this phase is to ensure and verify the overall RC frame behavior when modeled and retrofitted with BRB. The calibrated modeled BRB element of phase I is adopted in testing the retrofitted frames by BRB elements; some RC frames with different geometries and from various references are modeled using the SeismoStruct FE software program to carry out this phase.

4.1 Modeling Approach

The first experimental chosen program was that conducted by Pan et al.[18], the experimental study included testing the (WT-BS and WT-BD) specimens. The 'S' and 'D' letters stand for single and double constrained inner anchors. A steel frame is linked to the RC frame with single or double inner anchors. A single diagonal BRB element connecting its corners of 16 mm x 108 mm and 16 mm x 85 mm, respectively. The third one is the (specimen WT), which only consists of the RC frame with an installed steel frame, the 'WT' means the inclusion of four 100x200x8x12 mm WT shape members (A572 GR50 steel), all specimens have similar concrete dimensions and steel reinforcing details as shown in **Fig. 6**. The concrete column dimensions are 300 mm x 500 mm, the upper beam is 550 mm wide x 500 mm deep. The actual material strengthens can be summarized in**Table 5**.

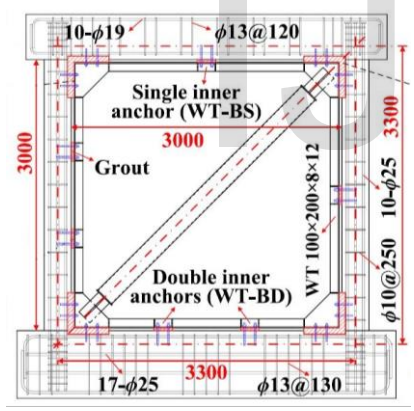

Fig. 6 Specimen details (Pan et al., 2016)

The validated frames are being modeled with the inelastic frame displacement-based (infrmDB) beam-column elements. The adopted material models are; "Mander et al." (con_ma) [26] for concrete, the "Menegotto-Pinto" steel model (stl_mp) [27] for the steel rebars, the "Bilinear Steel model" (stl_bl) for the WT steel members, and "Buckling Restrained Steel Brace model" (stl_brb) for the BRB elements.

Static pushover analysis is carried out, with the loading history as specified via the experimental program. As more drift ratio levels were conducted, to be more demanding than that of the AISC 360-10, starting from 0.125% and up to 5.0%, Three cycles were conducted for each drift level. However, in the FE simulation, the model structure is subjected to only one cycle of each drift level; due to the limitation of the displacement control phases number, also to decrease the computing time.

The second experimental chosen program was that conducted by Yooprasertchai et al. [13], the CBRB specimen is selected to be tested analytically. The modeling procedure goes through the same aforementioned procedure in the previous specimen, the same for the chosen material models. The loading protocol is conducted as offered by the experimental program.

Table 5 Actual Material Strengthens (Pan et al., 2016)

Column Reinforcing		Column Concrete	BRB core		WT member	
f_y (MPa)	f_u (MPa)	f_c (MPa)	f_y (MPa)	f_u (MPa)	f_y (MPa)	f_u (MPa)
468	671	25	397	530	394	483

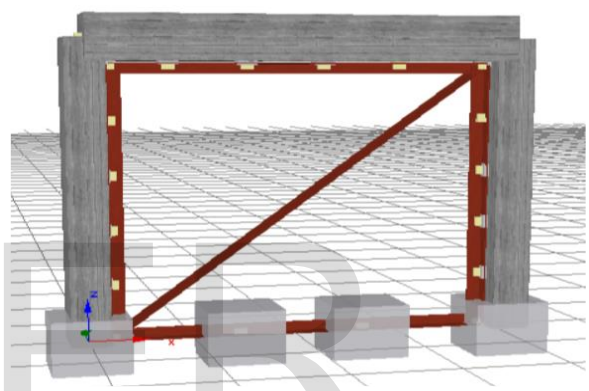

Fig. 7 WT-BD SeismoStruct model

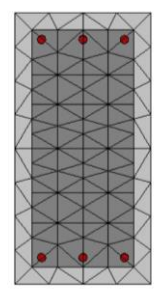

Fig. 8 Finite element mesh

4.2 In-frame (Phase II) Analytical Results

The main aim of this study is to find out a modeling technique that is both relevant and accurate for developing load-displacement relationships for the various previously stated experiments. The material models and specimens' geometry previously described in this paper are used in the generated study. The experimental cyclic analysis was utilized to test the analytically derived models.

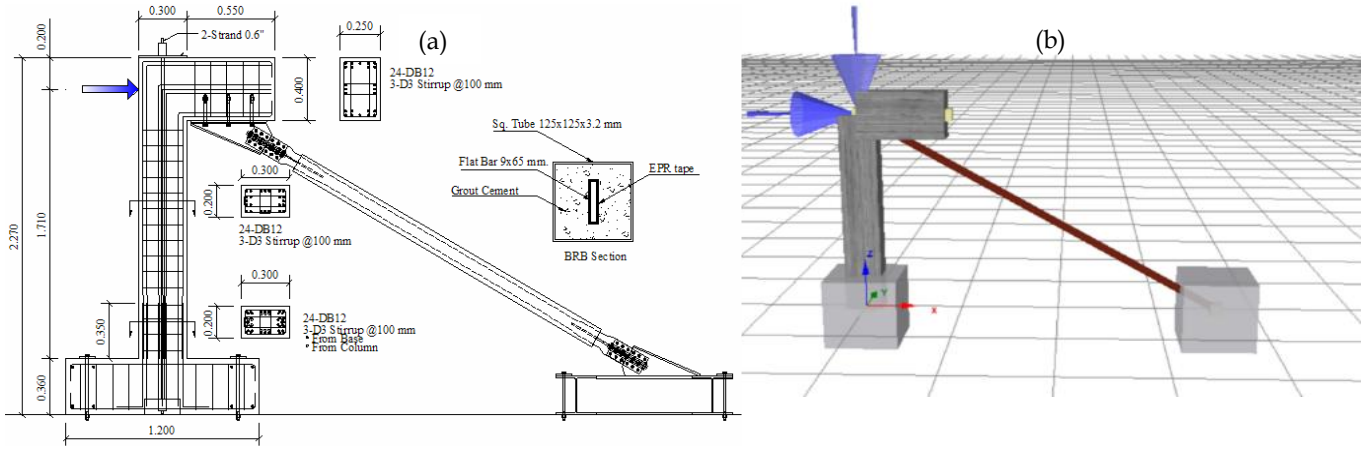

Fig. 9 CBRB specimen
(a) Specimen reinforcement details by (Yooprasertchai et al., 2008)
(b) SeismoStruct model

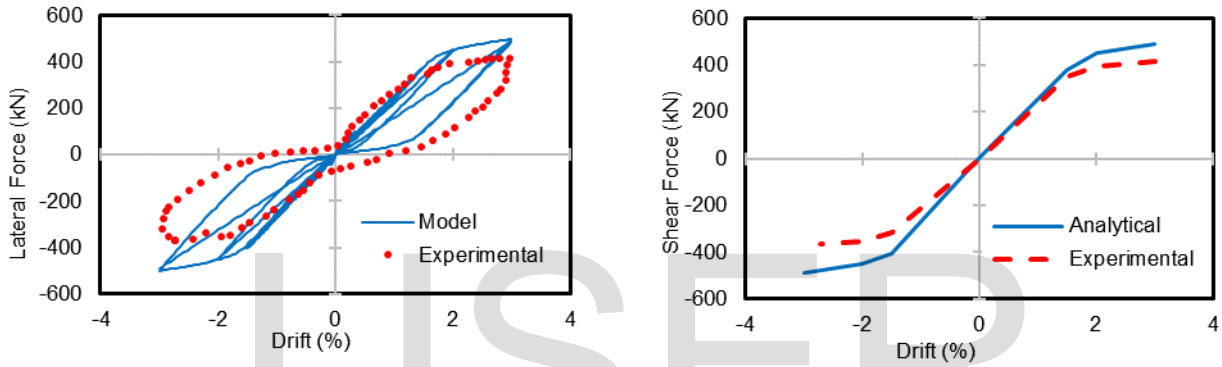

(a) WT Model (Pan et al. Model) Hysteresis Loops and Push-Pull Envelopes

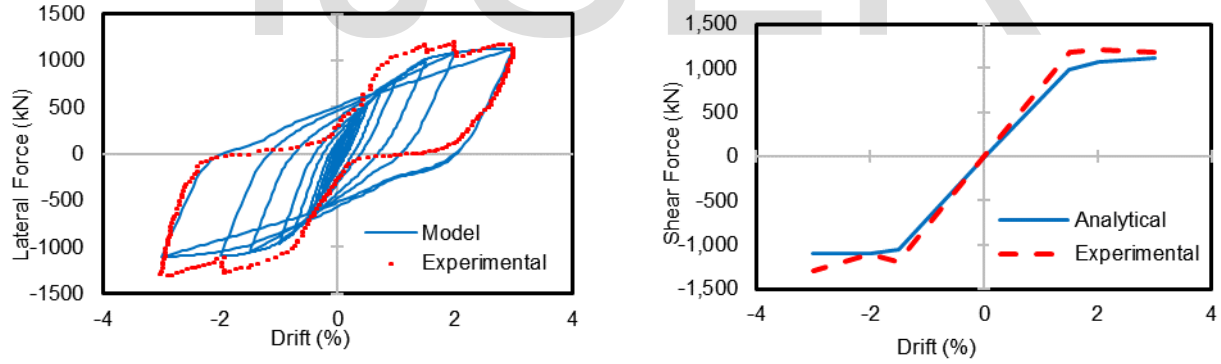

(b) WT-BS Model (Pan et al. Model) Hysteresis Loops and Push-Pull Envelopes

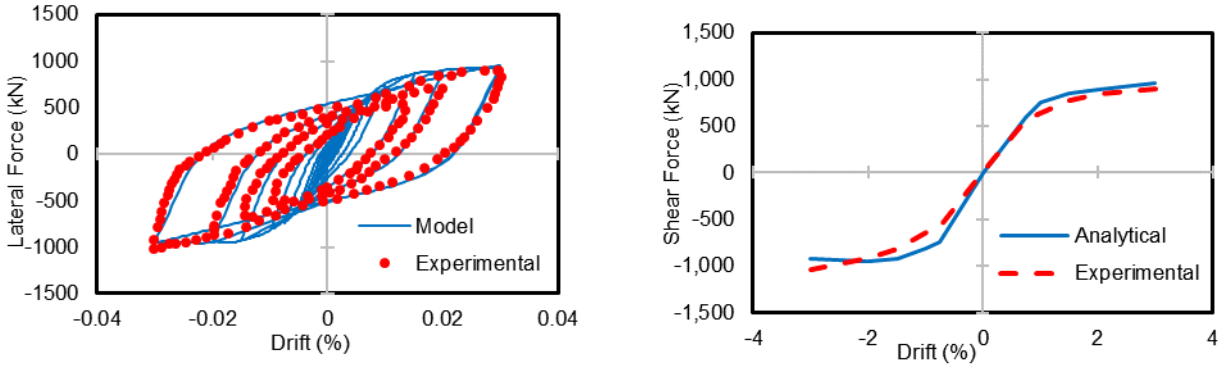

(c) WT-BD Model (Pan et al. Model) Hysteresis Loops and Push-Pull Envelopes

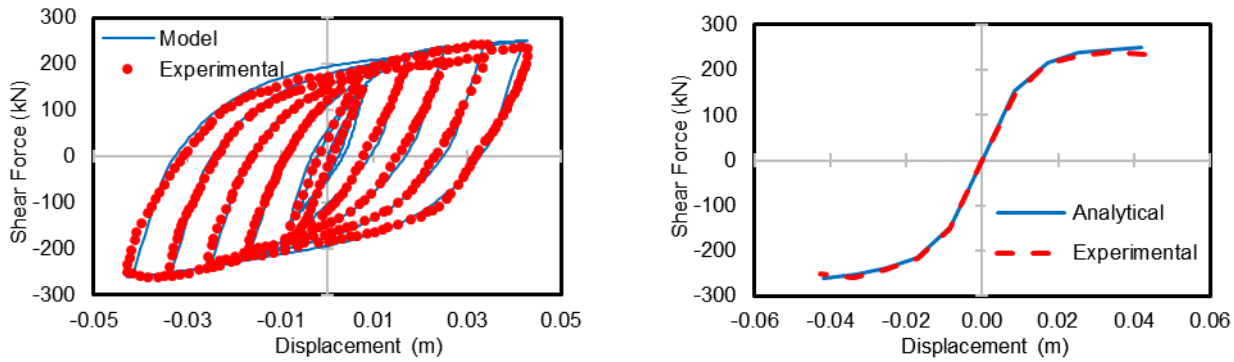

(d) CBRB Model (Yooprasertchai et al. Model) Hysteresis Loops and Push-Pull Envelopes

Fig. 10 Phase 2 Specimens Response Validation

The in-frame test results of phase II, show great matching results corresponding to the experimental results, interestingly for that BRB retrofitted especially (WT-BD and CBRB models), the mean difference observed for these two models for the peak strength was only 11% and 1%, for the effective stiffness only 11% and 2% respectively, for the energy dissipation 15% for the WT-BD and amazingly a zero% for the CBRB. The retrofitted modeled frames could be more assessed through the prescribed below tables in the following subsections.

The pinching behavior observed in the WT-BS specimen resulted from the load-bearing block crushing, which means spalling in the load transfer mechanism between the added steel members and the RC frame. Also, the single mid-span anchor used in the upper member failed, thus leading to buckling of the steel member. Such failures can not be predicted in the modeling simulation, leading to the results difference observed.

TABLE 6 demonstrates the difference between experimental and analytical values for the ultimate shear force. As well as the difference among the measured experimental and analytical values for shear force for all the five specimens. **TABLE 7** demonstrates the comparison among the experimental and analytical values for the displacement at ultimate shear strength.

4.2.1 Effective Stiffness and Energy dissipation

The k_{eff} and Ed are calculated as stated before in phase I. The results and comparisons are presented below. From the shown results, it can be said that both analytical keff and Ed are found slightly less than the experimental results, but with an acceptable percentage of less than 21%. Phase II results almost have the same trend for each of these parameters; which is similar to linear regression for the keff or progression for the Ed.

TABLE 6 SUMMARY OF EXPERIMENTAL AND ANALYTICAL ULTIMATE SHEAR FORCES

S.	Specimen	Experimental			Analytical			Difference
		Q_{u+ve}	Q_{u-ve}	Mean	Q_{u+ve}	Q_{u-ve}	Mean	
1	WT	415.77	-365.98	390.87	496.31	-498.48	497.40	27%
2	WT-BS	1209.13	-1304.11	1256.62	1129.05	-1105.32	1117.19	-11%
3	WT-BD	891.60	-1013.74	952.672	954.85	-958.55	956.70	0%
4	CBRB	242.33	-261.36	251.85	252.11	-262.08	257.10	2%

TABLE 7 SUMMARY OF EXPERIMENTAL AND ANALYTICAL DISPLACEMENTS AT ULTIMATE SHEAR STRENGTH

S.	Specimen	Experimental			Analytical			Difference
		Δ_{u+ve}	Δ_{u-ve}	Mean	Δ_{u+ve}	Δ_{u-ve}	Mean	
1	WT	0.092	-0.090	0.091	0.099	-0.099	0.099	9%
2	WT-BS	0.065	-0.096	0.080	0.099	-0.099	0.099	23%
3	WT-BD	0.089	-0.099	0.094	0.099	-0.073	0.086	-9%
4	CBRB	0.043	-0.042	0.042	0.043	-0.043	0.043	1%

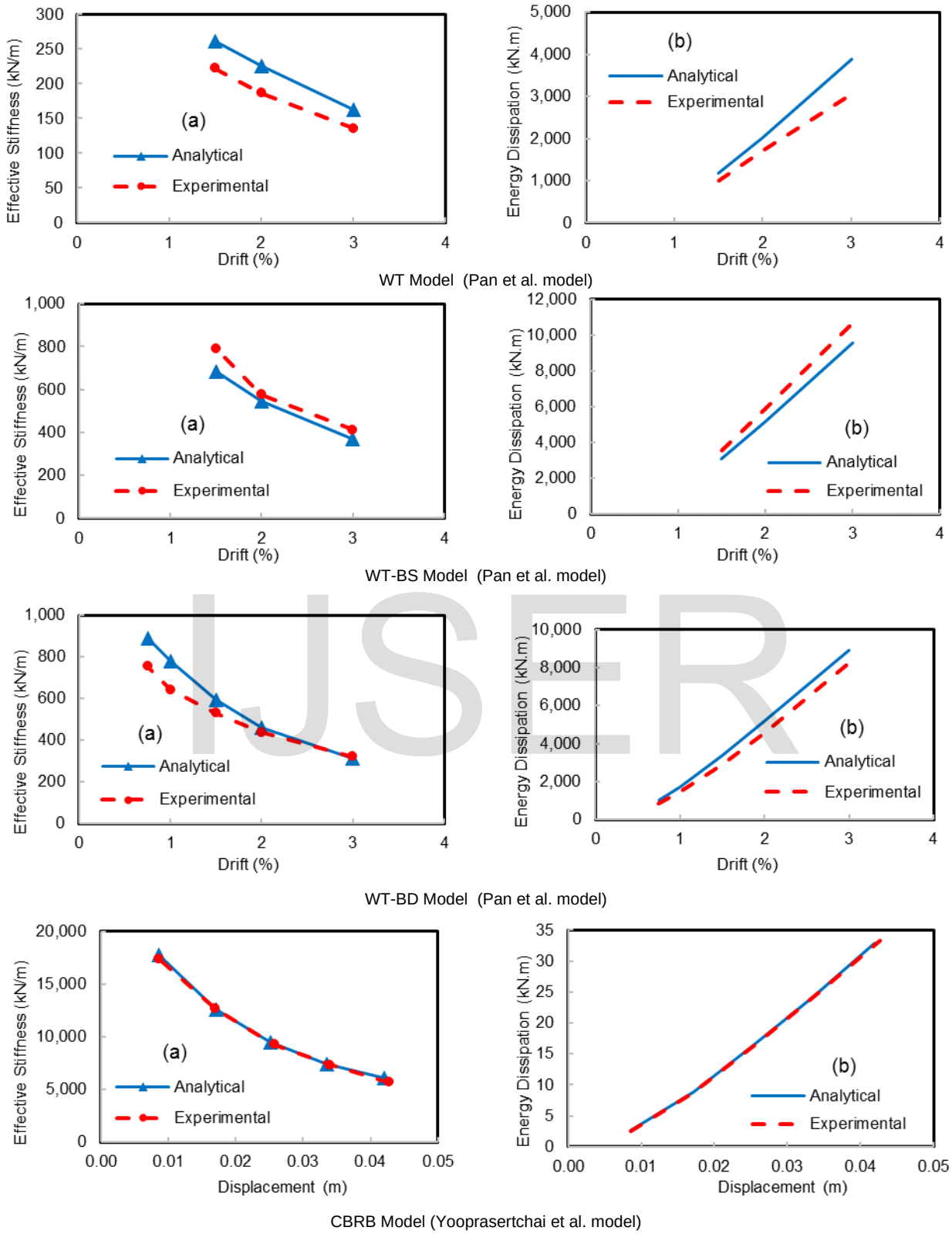

Fig. 11 Analytical vs Experimental Stiffness and Energy Dissipation Results
(a) Effective Stiffness; and (b) Energy Dissipation

Drift (%)	WT Specimen					
	Stiffness (kN/m)			Energy Dissipation (kN.m)		
	Analytical	Experimental	Difference	Analytical	Experimental	Difference
3	162.92	135.95	20%	1173.65	1001.40	17%
2	225.78	186.30	21%	2016.42	1707.80	18%
1.5	260.81	222.53	17%	3897.07	3037.44	28%
		Average	19%		Average	21%

Drift (%)	WT-BS Specimen					
	Stiffness (kN/m)			Energy Dissipation (kN.m)		
	Analytical	Experimental	Difference	Analytical	Experimental	Difference
3	371	411	-10%	3068	3562	-14%
2	543	577	-6%	5177	5904	-12%
1.5	682	792	-14%	9576	10680	-10%
		Average	-10%		Average	-12%

Drift (%)	WT-BD Specimen					
	Stiffness (kN/m)			Energy Dissipation (kN.m)		
	Analytical	Experimental	Difference	Analytical	Experimental	Difference
3	312	322	-3%	999.56	847.50	18%
2	458	437	5%	1722.79	1451.15	19%
1.5	592	530	12%	3391.55	2888.24	17%
1	780	642	21%	5196.88	4557.03	14%
0.75	888	753	18%	8901.07	8235.53	8%
		Average	11%		Average	15%

Drift (%)	CBRB Specimen					
	Stiffness (kN/m)			Energy Dissipation (kN.m)		
	Analytical	Experimental	Difference	Analytical	Experimental	Difference
0.0427	6089	5688	7%	2.60	2.54	2%
0.034	7407	7351	1%	8.87	8.70	2%
0.0257	9453	9252	2%	16.22	16.58	-2%
0.017	12592	12665	-1%	24.29	24.68	-2%
0.00855	17755	17403	2%	32.86	33.25	-1%
		Average	2%		Average	0%

5 Conclusions

The purpose of this research was to come up with a simple and reliable way to simulate the behavior of the BRB elements, either alone (component level) or mounted in an RC frame (system level). The load-displacement relationships generated for the individual BRB elements were incorporated into the full RC frame models. The analytical results were compared to the experimental ones. It was found that the model can capture the system behavior with acceptable accuracy. The results are collated and displayed in the preceding load-displacement relationships, indicating that the mismatching percentage is acceptable. As a result, it may be inferred that:

1) It is acceptable to model such the BRB elements by that way of modeling, using the prior stated class element and modeling technique.
2) The new material model (stl_brb) proposed by the FE software program, was very capable to predict the element behavior in both tension and compression sides.
3) Mander concrete model (con_ma) and Menegotto-Pinto

steel model (stl_mp) were very proper in modeling the behavior of reinforced concrete structures, as well as the Bilinear Steel model (stl_bl) for modeling the structural steel elements.

4) Utilizing the inelastic frame displacement-based (infrmDB) class element for all elements except for the braces while using the truss element for the braces gave good results and very close matching curve loops.
5) For capturing cyclic behavior, the modeling technique was proven to be satisfactory and computationally efficient. Such values for the factors governing the cyclic behavior of BRB steel material models were recommended.
6) Testing uniaxial BRB elements (Phase I) using the SeismoStruct FE software was able to capture their behavior in an acceptable percentage, with a mean difference of 5% for the cyclic response, 4% for the captured displacement at ultimate shear strength, 25% for effective stiffness, K_{eff}, and 22% for the energy dissipation, Ed.
7) The highest difference obtained from all BRB models at the component level, excluding the first specimen as it experienced experimental end rotation, for maximum shear force, and displacement at ultimate shear strength, were 9% and 8.4%, respectively.
8) Dividing the concrete elements and linking them with the inner steel frame provided better results than using the rigid offset option.
9) This modeling technique was able to capture the experimental results (of Phase II). For tests with no experimental failures, the highest mean difference obtained from all BRB models at the system level for maximum shear force, displacement at ultimate shear strength, effective stiffness, and energy dissipation were 4.7%, 6.1%, 6%, and 5.6%, respectively.
10) The highest difference obtained from all BRB models at the system level for maximum shear force, displacement at ultimate shear strength, effective stiffness, and energy dissipation was 27%, 23%, 21%, and 19%, respectively.
11) The results indicate that the stated analytical modeling technique can accurately predict the behavior of RC structures retrofitted with BRBs.
12) This study could be a start to generate a parametric study on RC buildings retrofitted with BRBs.

6 REFERENCES

[1] J. Lu, "Buckling mechanism of steel core and global stability design method for fixed-end buckling-restrained braces .pdf," *Eng. Struct.*, 2018.

[2] Clark P. Et al., "Large-scale testing of steel unbonded braces for energy dissipation, advanced technology in structural engineering," 2000.

[3] C. Uang, M. Nakashima, K. Tsai, and U. Chia-Ming, "Research and application of buckling-restrained braced frames," *Steel Structures*. pp. 301–313, 2004.

[4] P. Clark, I. Aiken, K. Kasai, E. Ko, and I. Kimura, "Design procedures for buildings incorporating hysteretic damping devices," *68th Annu. Conv. SEAOC*, pp. 355–371, 1999, [Online]. Available: http://eqstory.skku.ac.kr/05-OPEN-INFORM/CONTROL/SEAOC-PAPER/Hysteretic.pdf.

[5] R. A. Kersting, L. A. Fahnestock, and W. A. López, *Seismic Design of Steel Buckling- Restrained Braced Frames A Guide for Practicing Engineers*, no. 11. .

[6] S. Rafael, M. Stephen, and C. Chunho, "Seismic Demands on Steel Braced Frame Buildings with Buckling-Restrained Braces by Rafael Sabelli, Stephen Mahin and Chunho Chang," *Engineering*, pp. 1–20.

[7] Q. Xie, "State of the art of buckling-restrained braces in Asia," *J. Constr. Steel Res.*, vol. 61, no. 6, pp. 727–748, 2005, doi: 10.1016/j.jcsr.2004.11.005.

[8] D. Piedrafita, X. Cahis, E. Simon, and J. Comas, "A new modular buckling restrained brace for seismic resistant buildings," *Eng. Struct.*, vol. 56, pp. 1967–1975, 2013, doi: 10.1016/j.engstruct.2013.08.013.

[9] Star Seismic Europe Ltd., "Star Seismic Brochure - Buckling Restrained Brace," 2012.

[10] J. Kim and H. Choi, "Behavior and design of structures with buckling-restrained braces," *Eng. Struct.*, vol. 26, no. 6, pp. 693–706, 2004, doi: 10.1016/j.engstruct.2003.09.010.

[11] T. Takeuchi and A. Wada, "Review of buckling-restrained brace design and application to tall buildings," *Int. J. High-Rise Build.*, vol. 7, no. 3, pp. 187–195, 2018, doi: 10.21022/IJHRB.2018.7.3.187.

[12] A. Watanabe, "Design and applications of buckling-restrained braces," *Int. J. High-Rise Build.*, vol. 7, no. 3, pp. 215–221, 2018, doi: 10.21022/IJHRB.2018.7.3.215.

[13] E. Yooprasertchai and P. Warnitchai, "Seismic Retrofitting of Low-Rise Nonductile Reinforced Concrete Buildings By Buckling-Restrained Braces," 2008.

[14] L. Di Sarno and G. Manfredi, "Seismic retrofitting with buckling restrained braces: Application to an existing non-ductile RC framed building," *Soil Dyn. Earthq. Eng.*, vol. 30, no. 11, pp. 1279–1297, 2010, doi: 10.1016/j.soildyn.2010.06.001.

[15] S. Bordea and D. Dubina, "Retrofitting / upgrading of reinforced concrete elements with buckling restrained bracing elements," in *11th WSEAS International Conference on Sustainability in Science Engineering*, 2009, pp. 407–412.

[16] S. H. Saiful Islam, Matthew Skokan, "INNOVATIVE SEISMIC RETROFIT OF TWO HIGH-RISE BUILDINGS WITH UNIQUE CHALLENGES Saiful Islam 1 , MatthewSkokan 2 , Sampson Huang 3," 2010.

[17] Z. Qu, S. Kishiki, H. Sakata, A. Wada, and Y. Maida, "Subassemblage cyclic loading test of RC frame

with buckling restrained braces in zigzag configuration," *Earthq. Eng. Struct. Dyn.*, vol. 42, no. 7, pp. 1087–1102, 2013, doi: 10.1002/eqe.2260.

[18] K.-Y. Pan, "Seismic retrofit of reinforced concrete frames using buckling- restrained braces with bearing block load transfer mechanism," *Int. Assoc. Earthq. Eng.*, no. 056, pp. 1–6, 2016, doi: 10.1002/eqe.

[19] H. Abou-Elfath, M. Ramadan, and F. Omar Alkanai, "Upgrading the seismic capacity of existing RC buildings using buckling restrained braces," *Alexandria Eng. J.*, vol. 56, no. 2, pp. 251–262, 2017, doi: 10.1016/j.aej.2016.11.018.

[20] "Seismosoft," *SeismoStruct v2020-A computer program for static and dynamic nonlinear analysis of framaed structures.* http://www.seismosoft.com.

[21] A. Pavan, R. Pinho, and S. Antoniou, "Blind prediction of a full-scale 3d steel frame tested under dynamic conditions," *Earthquake*, no. Figure 1, pp. 0–7, 2008.

[22] G. L. Palazzo, P. Martín, F. Calderón, V. Roldán, and G. Maldonado, "Steel frame with buckling-restrained braces subject to near and far-fault inputs," *Building*, 2001.

[23] ASCE, "Minimum design loads for buildings and other structures," Reston, VA, 2010.

[24] T. L. Sinha B, Gerstle K, "Stress strain behavior for concrete under cyclic loading.," *Am Concr Inst Struct J*, no. 1964;61(2):195–211.

[25] S. F. Hose Y, "Performance evaluation database for concrete bridge components and systems under simulated seismic loads," 1999.

[26] P. R. Mander JB, Priestley MJN, "Theoretical stress-strain model for confined concrete.," *J Struct Eng*, pp. 114(8):1804–26, 1988.

[27] P. P. Menegotto M and and S. Engineering;, "Method of anaysis for cyclically loaded reinforced Behavior, concrete plane frames including changes in geometry and non-elastic Of, of elements under combined normal force and bending. Proc IABSE Symp Well-defined, resistance and ultimate deformability o," Libson, Portugal, 1973.